Turk J Elec Eng & Comp Sci, Vol.20, No.Sup.1, 2012, © TÜBİTAK
doi:10.3906/elk-1105-12

Voltage stability via energy function analysis on reduced order model of power system

Ahmet ÇİFCİ[1], Yılmaz UYAROĞLU[2,*], Mehmet Ali YALÇIN[2]
[1] *Department of Electrical and Energy, Mehmet Akif Ersoy University, Burdur-TURKEY*
e-mail: acifci@mehmetakif.edu.tr
[2] *Department of Electrical-Electronics Engineering, Sakarya University, Sakarya-TURKEY*
e-mails: uyaroglu@sakarya.edu.tr, yalcin@sakarya.edu.tr

Received: 06.05.2011

Abstract

A power system is a typical nonlinear dynamical system and voltage stability is an important subject of power system stability. This paper describes the use of the variable gradient method in a reduced order model of a single-machine infinite-bus power system. Additionally, the system's Lyapunov (energy) function is created and thus the system's energy level changes' effects on the system's stability are shown using the MACSYMA program. The Lyapunov function allows the determination of stability for nonlinear systems without the need to find exact solutions.

Key Words: *Lyapunov (Energy) function, reduced order model of single-machine infinite-bus power system, variable gradient method, voltage stability*

1. Introduction

Since the 1920s, electric power system stability has been considered as an important problem in terms of reliable system operation [1,2]. Consequently, many authors have been studying power system stability using different analyses [3-6]. Recently, voltage stability has become a basic issue in electric power systems because of the energy system collapses that have occurred in various places of the world such as Egypt [7], Chile [8], and the United States and Canada [9,10]. The concept of voltage stability is expressed as the ability of a power system to maintain steady voltage at all of the buses in the system after being subjected to a disturbance or contingency from a given initial operating condition [11].

In cases of not maintaining voltage control and an increase in the load due to disabling, for any reason, elements such as the generator, line, transformer, or bus if an uncontrolled voltage drop occurs, the result is power system instability. The main reason for voltage instability is that in an overloaded system, the system cannot ensure the reactive energy needed by the system to keep voltage values at a certain level [12-15]. Other

*Corresponding author: Department of Electrical and Energy, Mehmet Akif Ersoy University, Burdur-TURKEY

reasons are generator reactive power limits, load characteristics, characteristics of load tap changer transformer, characteristics of reactive power compensation devices, and behaviors of voltage control devices [16].

This paper is organized as follows: Section 2 outlines the main idea of Lyapunov stability analysis. In Section 3, we recall the single-machine infinite-bus (SMIB) power system considered in [17] and give a reduced order model of the SMIB power system considered in [18]. Section 4 examines the reduced order model's energy function. Section 5 presents simulation results of the energy function analysis. Finally, conclusions are given in Section 6.

2. Lyapunov stability analysis

The study of Lyapunov stability via energy functions has been applied in power systems [19-22]. The Lyapunov stability theory includes 2 methods, Lyapunov's first method and Lyapunov's second method (also called Lyapunov's direct method). Lyapunov's first method uses the linearization of a system to determine the local stability of the original system. Lyapunov's second method allows us to study the stability of the system concerning the dynamic system before finding the solution to the differential equation. The second method is appropriate for the voltage stability of nonlinear systems that do not have accurate solutions. This method is the most common one in terms of the determination of stability conditions of time-dependent nonlinear systems and could be applied to all known systems.

2.1. Stability analysis of nonlinear systems

Voltage stability of nonlinear systems is regional. Hence, the Lyapunov function, which obtains sufficient stability conditions in the largest region around the origin, is sought.

Some methods that arise from Lyapunov's second method are proper for examining the stability of nonlinear systems. One of them is the variable gradient method, which is used for the generalization of Lyapunov functions.

2.1.1. The variable gradient method

There are no generally applicable methods for finding Lyapunov functions. The variable gradient method provides a systematic approach to determining a suitable Lyapunov function. The variable gradient method assumes a certain form for the gradient of an unknown Lyapunov function, and then finds the Lyapunov function itself by integrating the assumed gradient [23].

Consider a nonlinear dynamical system described by:

$$\dot{x} = f(x,t). \tag{1}$$

Accept an equilibrium point at the origin of the space. Denote a test Lyapunov function by using V and its time derivative, $\dot{V}$. Assume that in Eq. (1), V is x's open function but not t's. Then,

$$\dot{V} = \frac{\partial V}{\partial x_1}\dot{x}_1 + \frac{\partial V}{\partial x_2}\dot{x}_2 + ... + \frac{\partial V}{\partial x_n}\dot{x}_n \tag{2}$$

can be written. Hence,

$$\dot{V} = (\nabla V)^* \dot{x}. \tag{3}$$

In Eq. (3), $(\nabla V)^*$ is ∇V's transpose. The gradient of V is denoted by ∇V, as follows:

$$\nabla V = \begin{bmatrix} \frac{\partial V}{\partial x_1} \\ . \\ . \\ . \\ \frac{\partial V}{\partial x_n} \end{bmatrix} = \begin{bmatrix} \nabla V_1 \\ . \\ . \\ . \\ \nabla V_n \end{bmatrix}. \tag{4}$$

∇V's line integral can be expressed by:

$$V = \int_0^x (\nabla V)^* dx. \tag{5}$$

In Eq. (5), the integral's upper limit does not point out that V is a vector magnitude, but the integral is preferred to the line integral of a random point (x_1,x_2,...,x_n) at the space. This integral can be done separately from the integration method.

2.1.2. Investigation of Lyapunov function using gradient system

A special class of dynamical system is particularly well suited to the Lyapunov method. This system arises from the gradient of a function [24]. A gradient dynamical system is given as:

$$\dot{x} = -A\nabla v(x, x_0). \tag{6}$$

In Eq. (6), v: $\Re^n x \Re^n \rightarrow \Re$ can be continuously differentiable. $A \in \Re^{nxn}$ is defined as det(A) $\neq$ 0 and v(x,x_0) = 0 for x = x_0. If v(x,x_0)'s Hessian is a completely positive definite at x_0, the equilibrium point is asymptotically stable at x_0. The Lyapunov function is given as:

$$V(x) = \int_{x_0}^x [f(\xi)]^T d\xi. \tag{7}$$

The Lyapunov function given above will be used in order to find the reduced order model of the SMIB power system's energy function.

3. The SMIB power system: the reduced order model

In this section, the SMIB power system is described [17,25]. First, a full order model is given, and then the resulting reduced order model is obtained.

3.1. The SMIB power system

We consider the power system model shown in Figure 1, which is taken from [17].

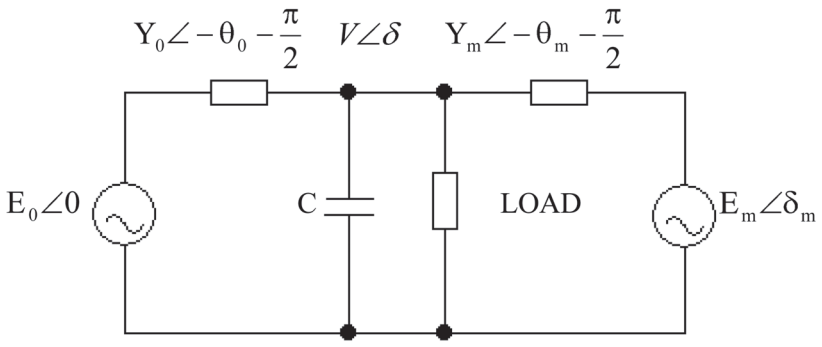

Figure 1. Power system model.

This system consists of a load bus and 2 generator buses. One of the generator buses is treated as a slack bus. The load is modeled by a simplified induction motor in parallel with a constant P-Q load and constant impedance. The load also includes a fixed capacitor, C, to raise the voltage up to near 1.0 per unit [17]. The network, load, and generator parameters are presented in the Appendix.

The active and reactive powers supplied to the load by the network are:

$$P = -E_0' V Y_0' \sin(\delta + \theta_0') - E_m V Y_m \sin(\delta - \delta_m + \theta_m) + (Y_0' \sin\theta_0' + Y_m \sin\theta_m) V^2, \tag{8}$$

$$Q = E_0' V Y_0' \cos(\delta + \theta_0') + E_m V Y_m \cos(\delta - \delta_m + \theta_m) - (Y_0' \cos\theta_0' + Y_m \cos\theta_m) V^2. \tag{9}$$

First order differential equations are expressed, which show the power system model's equations of state as follows [17]:

$$\dot{\delta}_m = w, \tag{10}$$

$$M\dot{w} = -Dw + P_m + E_m V Y_m \sin(\delta - \delta_m - \theta_m) + E_m^2 Y_m \sin\theta_m, \tag{11}$$

$$K_{qw}\dot{\delta} = -K_{qv} V - K_{qv2} V^2 + Q - Q_0 - Q_1, \tag{12}$$

$$TK_{qw}K_{pv}\dot{V} = K_{pw}K_{qv2}V^2 + (K_{pw}K_{qv} - K_{qw}K_{pv})V + K_{pw}(Q_0 + Q_1 - Q) - K_{qw}(P_0 + P_1 - P). \tag{13}$$

3.2. The reduced order model

The SMIB power system model presents significant numerical ill-conditioning. The dimensionality of this model is reduced by eliminating from it the variable δ, as considered in [18]. This is justified for the data used in [17], since K_{qw} is small in comparison with other system data [18]. The resulting reduced order model is:

$$\dot{\delta}_m = w, \tag{14}$$

$$M\dot{w} = -Dw + P_m + E_m V Y_m \sin(\delta - \delta_m - \theta_m) + E_m^2 Y_m \sin\theta_m, \tag{15}$$

$$TK_{pv}\dot{V} = -K_{pv} V - P_0 - P_1 + P. \tag{16}$$

4. Energy function of the reduced order model

The reduced order model differential equations above can be written again under the condition that the generator mechanical power is equivalent to the active load requirement ($\mathrm{P}_m = \mathrm{P}_l$).

$$\dot{w} = -\frac{D}{M^2}Mw - \frac{1}{M}f(\delta_m, V) \tag{17}$$

$$\dot{\delta}_m = \frac{1}{M}Mw \tag{18}$$

$$\dot{V} = -h(\delta_m, V) \tag{19}$$

Here,

$$f(\delta_m, V) = -(P_m + E_m V Y_m \sin(\delta - \delta_m - \theta_m) + E_m^2 Y_m \sin(\theta_m)), \tag{20}$$

$$h(\delta_m, V) = -\frac{1}{TK_{pv}}(-K_{pv}V - P_0 - P_1 + P). \tag{21}$$

4.1. Defining gradient system to the form of the Lyapunov function for the reduced order model

The derivation of the Lyapunov function for the reduced order model of the system in Figure 1 and Eqs. (17), (18), and (19) could be determined as:

$$\begin{bmatrix} \dot{\delta}_m \\ \dot{w} \\ \dot{V} \end{bmatrix} = \begin{bmatrix} 0 & -\frac{1}{M} & 0 \\ \frac{1}{M} & \frac{D}{M^2} & 0 \\ 0 & 0 & 1 \end{bmatrix} \begin{bmatrix} f(\delta_m, V) \\ Mw \\ h(\delta_m, V) \end{bmatrix}. \tag{22}$$

Eq. (22) for the reduced order model of the system defined in Eqs. (14), (15), and (16) is an alternative definition for this system's dynamics.

For (w_0, δ_{m0}, V_0)'s equilibrium point, a candidate energy function, which is seen on the right of Eq. (22) ((3 × 1) gradient matrix seen on the right of Eq. (22)), is obtained and thus can be used in Eq. (7). The candidate energy function can be written in Eq. (7) as:

$$v(w, \delta_m, V) = \int_{(w_0, \delta_{m0}, V_0)}^{(w, \delta_m, V)} \begin{bmatrix} Mx \\ f(\delta_m, V) \\ h(\delta_m, V) \end{bmatrix}^T \begin{bmatrix} dx \\ d\delta_m \\ dV \end{bmatrix}. \tag{23}$$

If f(w,δ_m,V) and h(w,δ_m,V) are replaced in Eq. (23), the reduced order model of the SMIB power system's energy function is obtained.

The equilibrium point is (w^*, δ_m^*, V^*) = (0.0, 0.3, 0.97).

5. Simulation results of the reduced order model

The generator rotor angle will be changed, beginning with 0, and will be increased to 1.6 by a 0.4 rise each turn in order to observe the reduced order model of the SMIB power system's stability. The sample of the energy function for the reduced order model is given as follows:

$$v(\delta, V) = -0.699V^3 + a_2V^2 + a_1V + a. \tag{24}$$

When the sample of the energy function given above is equalized, the reduced order model of the SMIB power system's energy function, which is obtained from Eq. (23), and a_2, a_1, and a are respectively obtained for each case.

The following cases are considered:

Case 1. Generator rotor angle $\delta_m = 0$ rad, system frequency w = 1 per unit (p.u.).

a_2, a_1, and a are respectively obtained as:

$$a_2 = -0.15 - 10\sin(\delta - 0.209) - 2.5\sin(\delta - 0.087), \tag{25}$$

$$a_1 = -0.6 + 5\cos(\delta - 0.213) - 5\cos(\delta + 0.087), \tag{26}$$

$$a = 1.379 + 9.409\sin(\delta - 0.209) + 2.352\sin(\delta - 0.087). \tag{27}$$

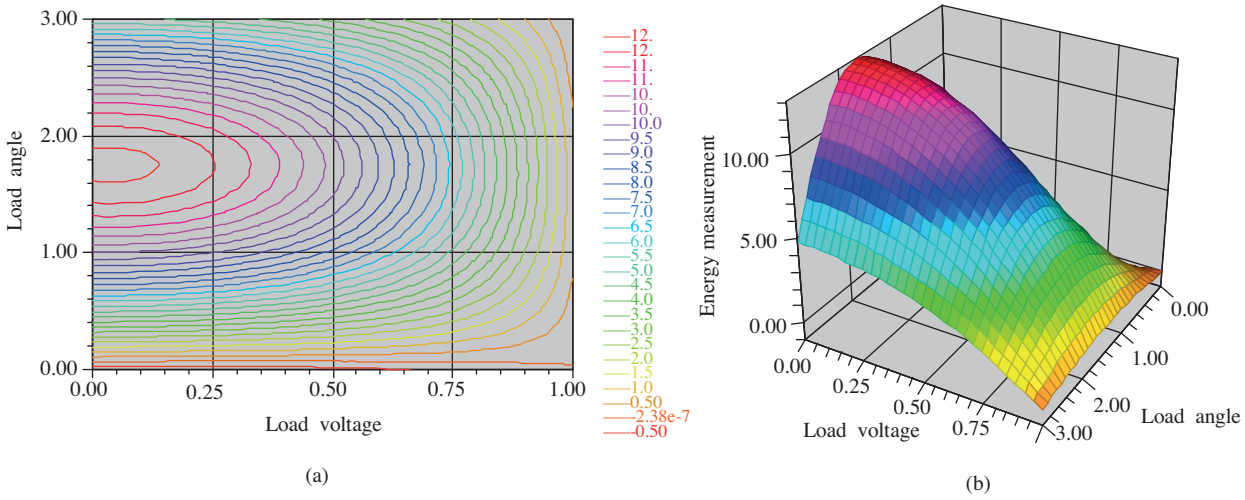

Figure 2. The reduced order model's stored energy for $\delta_m = 0$: (a) 2-dimensional representation and (b) 3-dimensional representation.

The reduced order model's energy density is in the range of $0 \leq$ V ≤ 0.3 and $1.4 \leq \delta \leq 1.8$, which is seen in Figure 2 and Table 1. The reduced order model's energy density varies between 12 and 13 energy units around these points.

For $\delta_m = 0$ rad and w = 1 p.u., Table 1 shows the numerical values of the energy function for different load angles and different load voltages.

Table 1. Energy measurement for $\delta_m = 0$.

δ					Energy measurement						
0	–0.8	–0.8	–0.8	–0.8	–0.8	–0.7	–06	–0.5	–0.3	–0.2	0.0
0.2	1.6	1.5	1.5	1.4	1.3	1.2	1.0	0.9	0.7	0.4	0.1
0.4	3.9	3.9	3.8	3.6	3.4	3.0	2.7	2.2	1.6	1.0	0.3
0.6	6.1	6.1	5.9	5.7	5.3	4.8	4.2	3.5	2.6	1.6	0.4
0.8	8.2	8.1	7.9	7.6	7.1	6.4	5.6	4.6	3.4	2.1	0.5
1	9.9	9.9	9.7	9.3	8.7	7.8	6.8	5.6	4.1	2.5	0.6
1.2	11.4	11.3	11.1	10.6	9.9	9.0	7.8	6.4	4.7	2.8	0.7
1.4	12.4	12.4	12.1	11.6	10.8	9.8	8.5	6.9	5.1	3.0	0.7
1.6	13.0	12.9	12.7	12.1	11.3	10.2	8.9	7.3	5.4	3.2	0.7
1.8	13.1	13.1	12.8	12.2	11.4	10.3	8.9	7.3	5.4	3.2	0.7
V	0	0.1	0.2	0.3	0.4	0.5	0.6	0.7	0.8	0.9	1

Case 2. Generator rotor angle $\delta_m = 0.4$ rad, system frequency w = 1 p.u.
a_2, a_1, and a are respectively obtained as:

$$a_2 = -0.15 - 10\sin(\delta - 0.209) - 2.5\sin(\delta - 0.487), \tag{28}$$

$$a_1 = -0.6 + 5\cos(\delta - 0.213) - 5\cos(\delta - 0.313), \tag{29}$$

$$a = 1.153 + 9.409\sin(\delta - 0.209) + 2.352\sin(\delta - 0.487). \tag{30}$$

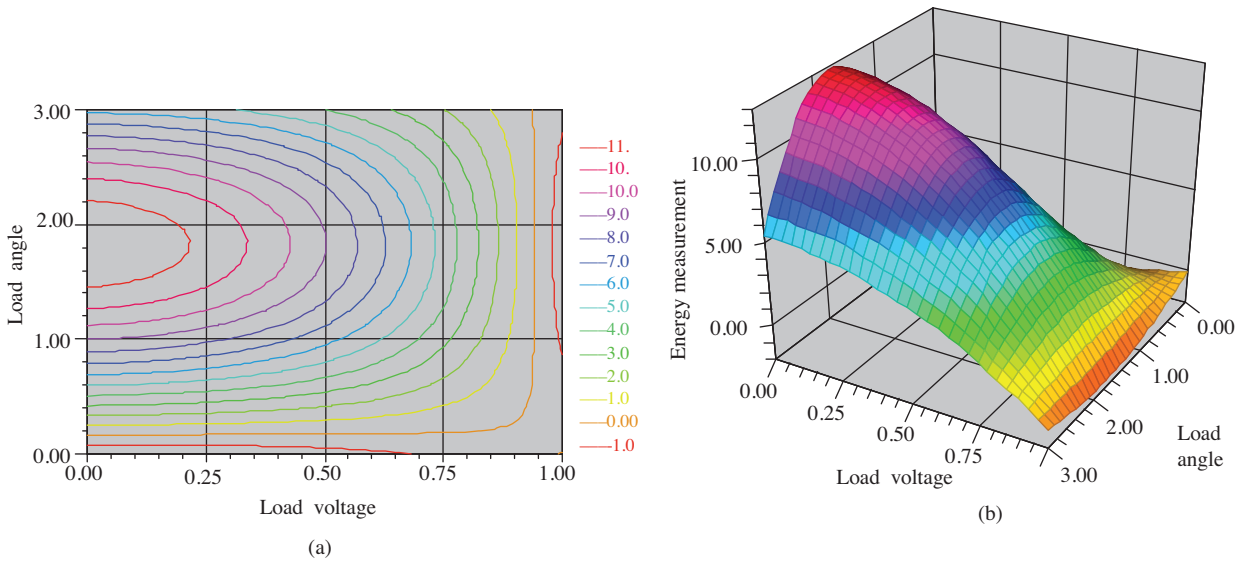

Figure 3. The reduced order model's stored energy for $\delta_m = 0.4$: (a) 2-dimensional representation and (b) 3-dimensional representation.

The reduced order model's energy density is in the range of $0 \leq V \leq 0.3$ and $1.4 \leq \delta \leq 1.8$, which is seen in Figure 3 and Table 2. The reduced order model's energy density varies between 11 and 12 energy units around these points.

Table 2. Energy measurement for $\delta_m = 0.4$.

δ					Energy measurement						
0	–1.9	–1.9	–1.9	–1.8	–1.6	–1.4	–1.2	–1.0	–0.7	–0.3	0.0
0.2	0.4	0.4	0.3	0.3	0.2	0.2	0.1	0.1	0.0	–0.1	–0.2
0.4	2.7	2.6	2.5	2.4	2.1	1.9	1.5	1.1	0.7	0.1	–0.5
0.6	5.0	4.9	4.7	4.4	4.0	3.5	2.9	2.2	1.3	0.4	–0.7
0.8	7.1	7.0	6.7	6.3	5.7	5.0	4.1	3.1	1.9	0.6	–0.9
1	9.0	8.8	8.5	7.9	7.2	6.3	5.2	3.9	2.5	0.8	–1.1
1.2	10.6	10.4	10.0	9.3	8.5	7.4	6.2	4.6	2.9	0.9	–1.3
1.4	11.8	11.5	11.1	10.4	9.5	8.3	6.9	5.2	3.2	1.0	–1.4
1.6	12.5	12.3	11.8	11.1	10.1	8.8	7.3	5.5	3.5	1.1	–1.5
1.8	12.8	12.6	12.1	11.4	10.3	9.1	7.5	5.7	3.6	1.2	–1.5
V	0	0.1	0.2	0.3	0.4	0.5	0.6	0.7	0.8	0.9	1

For $\delta_m = 0.4$ rad and w = 1 p.u., Table 2 shows the numerical values of the energy function for different load angles and different load voltages.

Case 3. Generator rotor angle $\delta_m = 0.8$ rad, system frequency w = 1 p.u.

a_2, a_1, and a are respectively obtained as:

$$a_2 = -0.15 - 10\sin(\delta - 0.209) - 2.5\sin(\delta - 0.887), \tag{31}$$

$$a_1 = -0.6 + 5\cos(\delta - 0.213) - 5\cos(\delta - 0.713), \tag{32}$$

$$a = 0.927 + 9.409\sin(\delta - 0.209) + 2.352\sin(\delta - 0.887). \tag{33}$$

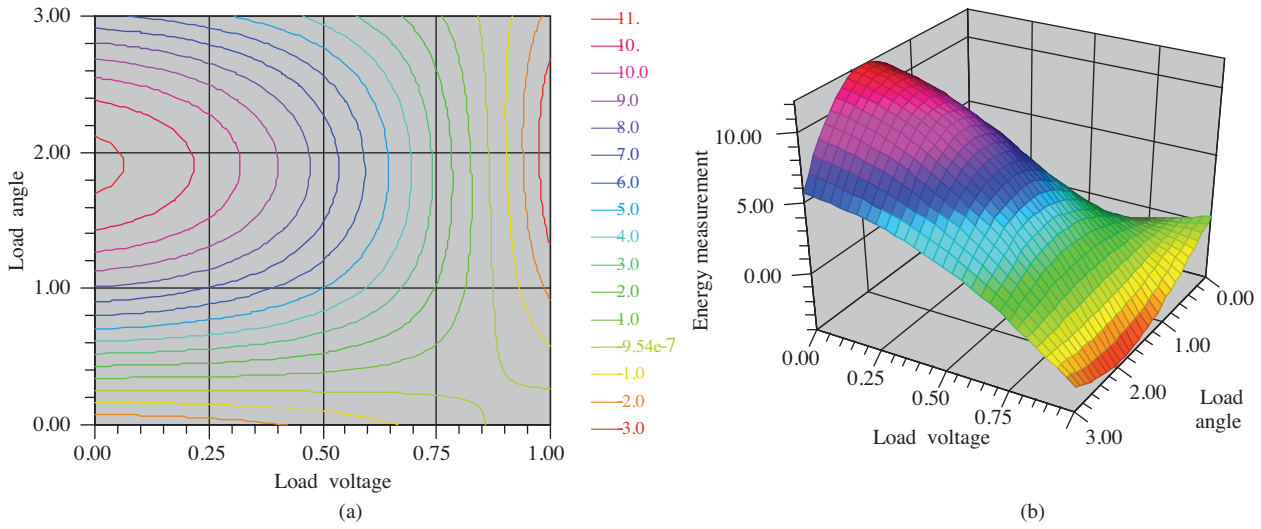

Figure 4. The reduced order model's stored energy for $\delta_m = 0.8$: (a) 2-dimensional representation and (b) 3-dimensional representation.

The reduced order model's energy density is in the range of $0 \leq V \leq 0.2$ and $1.6 \leq \delta \leq 1.8$, which is seen in Figure 4 and Table 3. The reduced order model's energy density varies between 11 and 12 energy units around these points.

Table 3. Energy measurement for $\delta_m = 0.8$.

δ					Energy Measurement						
0	–2.8	–2.8	–2.6	–2.4	–2.1	–1.7	–1.3	–0.8	–0.3	0.2	0.8
0.2	–0.6	–0.6	–0.6	–0.5	–0.4	–0.3	–0.2	–0.1	0.0	0.1	0.2
0.4	1.6	1.6	1.5	1.4	1.2	1.1	0.9	0.6	0.3	0.0	–0.4
0.6	3.8	3.7	3.5	3.3	2.9	2.5	2.0	1.4	0.7	–0.1	–1.0
0.8	6.0	5.8	5.5	5.0	4.5	3.8	3.0	2.0	1.0	–0.3	–1.7
1	7.9	7.6	7.2	6.6	5.9	5.0	3.9	2.6	1.2	–0.4	–2.2
1.2	9.5	9.2	8.7	8.0	7.1	6.0	4.7	3.1	1.4	–0.5	–2.7
1.4	10.8	10.5	9.9	9.1	8.0	6.8	5.3	3.5	1.6	–0.7	–3.1
1.6	11.7	11.3	10.7	9.8	8.7	7.3	5.7	3.8	1.7	–0.8	–3.4
1.8	12.2	11.8	11.1	10.2	9.0	7.6	5.9	3.9	1.7	–0.8	–3.6
V	0	0.1	0.2	0.3	0.4	0.5	0.6	0.7	0.8	0.9	1

For $\delta_m = 0.8$ rad and w = 1 p.u., Table 3 shows the numerical values of the energy function for different load angles and different load voltages.

Case 4. Generator rotor angle $\delta_m = 1.2$ rad, system frequency w = 1 p.u.

a_2, a_1, and a are respectively obtained as:

$$a_2 = -0.15 - 10\sin(\delta - 0.209) - 2.5\sin(\delta - 1.287), \tag{34}$$

$$a_1 = -0.6 + 5\cos(\delta - 0.213) - 5\cos(\delta - 1.113), \tag{35}$$

$$a = 0.701 + 9.409\sin(\delta - 0.209) + 2.352\sin(\delta - 1.287). \tag{36}$$

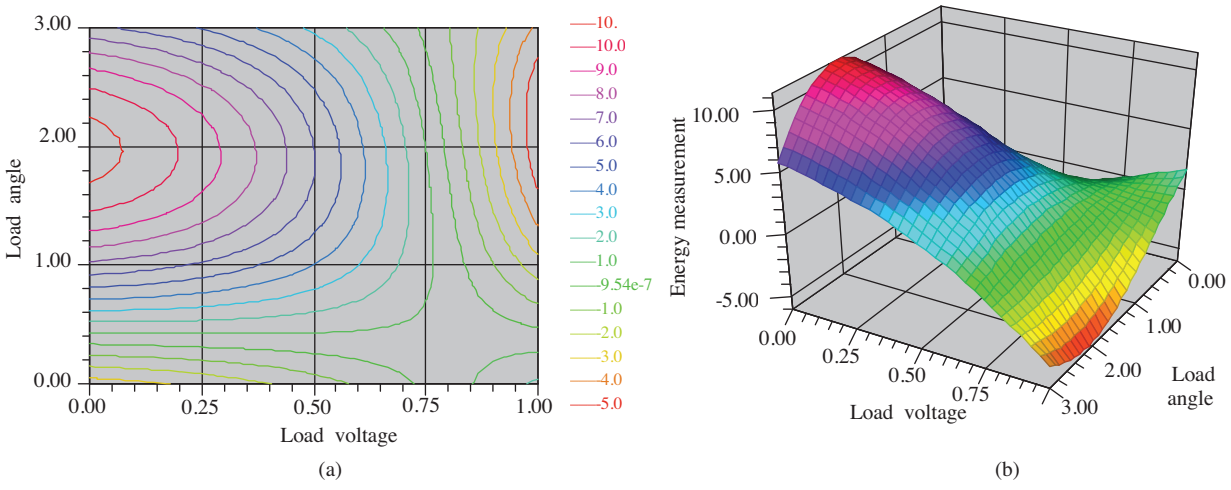

Figure 5. The reduced order model's stored energy for $\delta_m = 1.2$: (a) 2-dimensional representation and (b) 3-dimensional representation.

The reduced order model's energy density is in the range of $0 \leq V \leq 0.2$ and $1.4 \leq \delta \leq 1.8$, which is seen in Figure 5 and Table 4. The reduced order model's energy density varies between 9 and 10 energy units around these points.

Table 4. Energy measurement for $\delta_m = 1.2$.

δ					Energy measurement						
0	–3.5	–3.3	–2.9	–2.5	–2.0	–1.5	–0.9	–0.2	0.6	1.4	2.2
0.2	–1.5	–1.3	–1.1	–0.9	–0.6	–0.3	0.0	0.3	0.6	1.0	1.3
0.4	0.7	0.7	0.8	0.8	0.8	0.8	0.8	0.7	0.7	0.5	0.4
0.6	2.8	2.7	2.6	2.5	2.2	2.0	1.6	1.2	0.7	0.1	–0.6
0.8	4.8	4.7	4.4	4.1	3.6	3.0	2.3	1.5	0.6	–0.4	–1.6
1	6.7	6.5	6.1	5.5	4.8	4.0	3.0	1.8	0.5	–0.9	–2.6
1.2	8.4	8.0	7.5	6.8	5.9	4.8	3.5	2.1	0.4	–1.4	–3.5
1.4	9.7	9.3	8.6	7.8	6.7	5.4	3.9	2.2	0.3	–1.8	–4.2
1.6	10.7	10.2	9.4	8.5	7.3	5.9	4.2	2.3	0.2	–2.2	–4.9
1.8	11.3	10.7	9.9	8.9	7.6	6.1	4.3	2.3	0.0	–2.6	–5.4
V	0	0.1	0.2	0.3	0.4	0.5	0.6	0.7	0.8	0.9	1

For $\delta_m = 1.2$ rad and w = 1 p.u., Table 4 shows the numerical values of the energy function for different load angles and different load voltages.

Case 5. Generator rotor angle $\delta_m = 1.6$ rad, system frequency w = 1 p.u.

a_2, a_1, and a are respectively obtained as:

$$a_2 = -0.15 - 10\sin(\delta - 0.209) - 2.5\sin(\delta - 1.687), \tag{37}$$

$$a_1 = -0.6 + 5\cos(\delta - 0.213) - 5\cos(\delta - 1.513), \tag{38}$$

$$a = 0.474 + 9.409\sin(\delta - 0.209) + 2.352\sin(\delta - 1.687). \tag{39}$$

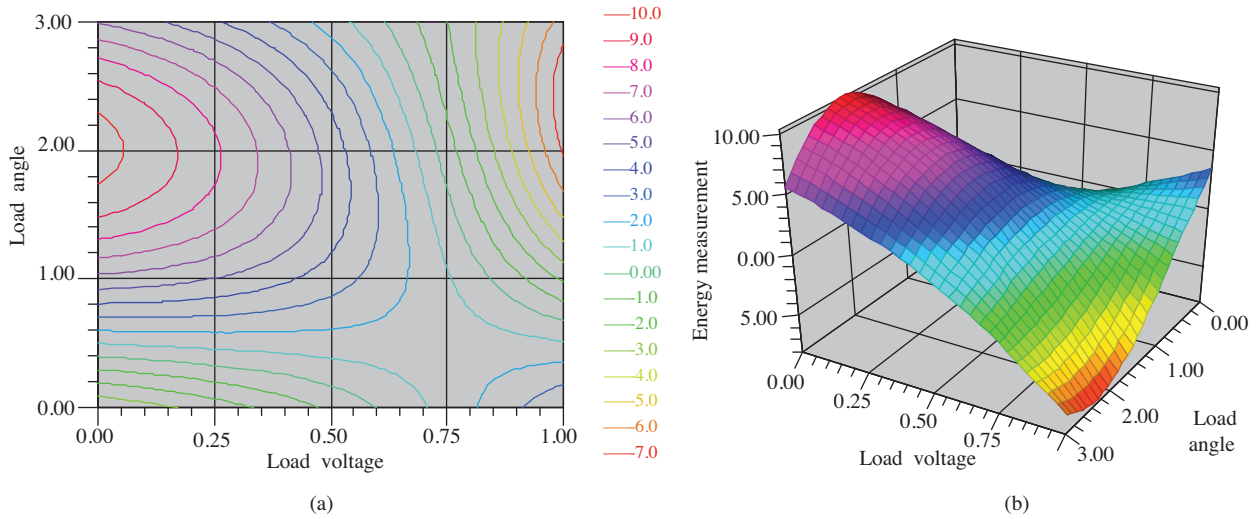

Figure 6. The reduced order model's stored energy for $\delta_m = 1.6$: (a) 2-dimensional representation and (b) 3-dimensional representation.

The reduced order model's energy density is in the range of $0 \leq V \leq 0.1$ and $1.6 \leq \delta \leq 1.8$, which is seen in Figure 6 and Table 5. The reduced order model's energy density varies between 9 and 10 energy units around these points.

Table 5. Energy measurement for $\delta_m = 1.6$.

δ					Energy measurement						
0	–3.8	–3.4	–2.8	–2.2	–1.6	–0.8	0.0	0.9	1.8	2.8	3.9
0.2	–2.0	–1.6	–1.2	–0.8	–0.4	0.1	0.6	1.2	1.7	2.3	2.9
0.4	0.0	0.2	0.4	0.6	0.9	1.1	1.2	1.4	1.6	1.7	1.8
0.6	2.0	2.1	2.1	2.1	2.0	1.9	1.8	1.6	1.3	0.9	0.5
0.8	3.9	3.8	3.7	3.5	3.2	2.8	2.2	1.6	0.9	0.1	–0.8
1	5.7	5.5	5.2	4.7	4.2	3.5	2.6	1.7	0.5	–0.7	–2.1
1.2	7.2	6.9	6.4	5.8	5.0	4.0	2.9	1.6	0.1	–1.6	–3.4
1.4	8.5	8.1	7.5	6.6	5.6	4.4	3.0	1.4	–0.4	–2.4	–4.6
1.6	9.5	9.0	8.2	7.2	6.1	4.7	3.1	1.2	–0.8	–3.1	–5.6
1.8	10.1	9.5	8.6	7.5	6.2	4.7	3.0	1.0	–1.3	–3.7	–6.5
V	0	0.1	0.2	0.3	0.4	0.5	0.6	0.7	0.8	0.9	1

For $\delta_m = 1.6$ rad and w = 1 p.u., Table 5 shows the numerical values of the energy function for different load angles and different load voltages.

After all of these cases, we observed that the value of the whole energy density decreased. This decrease in energy measurement is an indicator of the operating point's movement toward the instability region. In Case 1, while $\delta = 1.8$ rad and V = 0 p.u., the maximum energy level was 13.1 energy units. However, in Case 5, the energy level was 10.1 energy units, even with the same values of δ and V. It is observed clearly that any changes in load will continue to decrease the level of energy density to low values, and it is even possible to see negative values.

6. Conclusion

Energy function has long been recognized as a useful way of analyzing voltage stability. This paper demonstrated that a more realistic energy function, which can clearly demonstrate the critical load angles gained on the energy measurement levels, corresponding to the representations of system works in the different levels and load voltages, and the reduced order model of the SMIB power system's stability attitude, can be obtained. Thus, this shows the effect of energy fluctuations in the system on system stability, nearly definitely. Eventually, for the system dependency of load angle and load voltage, the optimal range of load angle and load voltage can be defined with the energy fluctuation that is plotted on the range of stability shown.

Appendix

The load parameter values used in the simulation are [17]:

$$K_{pv} = 0.3, T = 8.5, P_0 = 0.6, Q_0 = 1.3, P_1 = 0.0, Q_1 = 0.0.$$

The network and generator parameter values used in the simulation are [17]:

$$Y_0 = 20, \theta_0 = -5, E_0 = 1, C = 12, Y_0' = 8, \theta_0' = -12, E_0' = 2.5, Y_m = 5, \theta_m = -5, E_m = 1, P_m = 1,$$

$$D = 0.05, M = 0.3.$$

All of the values are given per unit (p.u.) except for angles, which are in degrees.

List of Symbols

δ	Load angle, rad
V	Load voltage, p.u.
w	Angular speed, rad/s
E_m	Generator voltage, p.u.
E_0	Infinite bus or slack bus voltage, p.u.
Y_m	Generator admittance, p.u.
Y_0	Infinite bus or slack bus admittance, p.u.
δ_m	Generator rotor angle, rad
C	Compensated load capacitor, p.u.
θ_m	Generator admittance angle, degrees
θ_0	Infinite bus admittance angle, degrees
M	Generator inertia, p.u.
D	Damping coefficient
T	Characteristic time constant of the motor, p.u.
P_0, Q_0	Constant real and reactive powers of the motor, p.u.
P_1, Q_1	Constant P-Q load, p.u.
P_m	Mechanical power, p.u.
$K_{pw}, K_{pv}, \ K_{qw}, K_{qv}, K_{qv2}$	Constant parameters

References

[1] C.P. Steinmetz, "Power control and stability of electric generating stations", Transactions of the American Institute of Electrical Engineers, Vol. 39, pp. 1215-1287, 1920.

[2] AIEE Subcommittee on Interconnections and Stability Factors, "First report of power system stability", Transactions of the American Institute of Electrical Engineers, Vol. 56, pp. 51-80, 1926.

[3] K. Kobravi, W. Kinsner, S. Filizadeh, "Analysis of bifurcation and stability in a simple power system using MATCONT", The 20th IEEE Canadian Conference on Electrical and Computer Engineering, pp. 1150-1154, 2007.

[4] V. Spitsa, A. Alexandrovitz, E. Zeheb, "Voltage stability analysis of power system with uncertain load characteristics", Proceedings of the World Automation Congress, pp. 137-142, 2004.

[5] P. Li, B.H. Zhang, J. Shu, Z.Q. Bo, A. Klimek, "Research on order reduction of power system modeling for dynamic voltage stability analysis", IEEE Transmission and Distribution Conference and Exposition, pp. 1-5, 2010.

[6] İ. Genç, Ö. Usta, "Impacts of distributed generators on the oscillatory stability of interconnected power systems", Turkish Journal of Electrical Engineering & Computer Sciences, Vol. 13, pp. 149-161, 2005.

[7] M.Z. El-Sadek, "Preventive measures for voltage collapses and voltage failures in the Egyptian power system", Electric Power Systems Research, Vol. 44, pp. 203-211, 1998.

[8] L.S. Vargas, C.A. Canizares, "Time dependence of controls to avoid voltage collapse", IEEE Transactions on Power Systems, Vol. 15, pp. 1367-1375, 2000.

[9] John F. Kennedy School of Government, Causes of the August 14th Blackout in The United States and Canada, Tech. Rep., Boston, Harvard University, 2003.

[10] US-Canada Power System Outage Task Force, First Report on the August 14, 2003, Blackout in the United States and Canada: Causes and Recommendations, Washington DC, US Department of Energy, 2004.

[11] P. Kundur, Power System Stability and Control, Toronto, McGraw-Hill, 1994.

[12] IEEE Working Group on Voltage Stability, "Voltage stability of power system: concepts, analytical tools, and industry experience", IEEE Special Publication, Paper 90TH0358-2-PWR, 1990.

[13] T. Van Cutsem, "Voltage instability: phenomena, countermeasures and analysis methods", Proceedings of the IEEE, Vol. 88, pp. 208-227, 2000.

[14] D.J. Hill, "Nonlinear dynamic load models with recovery for voltage stability studies", IEEE Transactions on Power Systems, Vol. 8, pp. 166-176, 1993.

[15] T. Van Cutsem, C. Vournas, Voltage Stability of Electric Power Systems, Norwell, Massachusetts, Kluwer Academic Publishers, 1998.

[16] J. Viswanatha Rao, S. Sivanagaraju, "Voltage regulator placement in radial distribution system using discrete particle swarm optimization", International Review of Electrical Engineering, Vol. 3, pp. 525-531, 2008.

[17] H.D. Chiang, I. Dobson, R.J. Thomas, J.S. Thorp, L. Fekih-Ahmed, "On voltage collapse in electric power systems", IEEE Transactions on Power Systems, Vol. 5, pp. 601-611, 1990.

[18] E.H. Abed, J.C. Alexander, H. Wang, A.M.A. Hamdan, H.C. Lee, "Dynamic bifurcations in a power system model exhibiting voltage collapse", Technical Research Report TR 92-26, Systems Research Center, University of Maryland, 1992.

[19] A. Çifci, Y. Uyaroğlu, A.T. Hocaoğlu, "Voltage stability analysis using the variable gradient method", International Review of Electrical Engineering, Vol. 6, pp. 914-921, 2011.

[20] Y. Chen, K. Zhou, "A new energy function based power system stability control scheme using real-time data", Proceedings of the International Conference on Power System Technology, pp. 163-168, 2000.

[21] I.A. Hiskens, R.J. Davy, "Lyapunov function analysis of power systems with dynamic loads", Proceedings of the 35th Conference on Decision and Control, pp. 3870-3875, 1996.

[22] F. Jurado, J. Carpio, "Energy functions analysis in voltage collapse", European Transactions on Electrical Power, Vol. 11, pp. 235-240, 2001.

[23] J.J.E. Slotine, W. Li, Applied Nonlinear Control, New Jersey, Prentice Hall, 1991.

[24] E.R. Scheinerman, Invitation to Dynamical Systems, New Jersey, Prentice Hall, 2000.

[25] A. Sedaghati, "A PI controller based on gain-scheduling for synchronous generator", Turkish Journal of Electrical Engineering & Computer Sciences, Vol. 14, pp. 241-251, 2006.